Mutation altering the miR-184 seed region causes keratoconus with cataract

Hughes, A., Bradley, D., Campbell, M., Lechner, J., Dash, D., Simpson, D., & Willoughby, C. (2011). Mutation altering the miR-184 seed region causes keratoconus with cataract. *The American Journal of Human Genetics*, *89*(5), 628-633. https://doi.org/10.1016/j.ajhg.2011.09.014

Published in:
The American Journal of Human Genetics

Document Version:
Peer reviewed version

Queen's University Belfast - Research Portal:
Link to publication record in Queen's University Belfast Research Portal

Mutation altering the miR-184 seed region causes familial keratoconus with cataract

Anne E. Hughes[1,3]*, Declan T. Bradley[1,3], Malcolm Campbell[1], Judith Lechner[2], Durga P. Dash[2], David A. Simpson[2] and Colin E. Willoughby[2]

[1]Centre for Public Health, The Queen's University of Belfast, Royal Victoria Hospital, Grosvenor Road, Belfast BT12 6BN, Northern Ireland, UK

[2]Centre for Vision and Vascular Science, The Queen's University of Belfast, Royal Victoria Hospital, Grosvenor Road, Belfast BT12 6BA, Northern Ireland, UK

[3]These authors contributed equally to this work

*To whom correspondence should be addressed (A.Hughes@qub.ac.uk)

Address:

Centre for Public Health

The Queen's University of Belfast

Institute of Clinical Sciences 'B'

Royal Victoria Hospital

Grosvenor Road

Belfast BT12 6BN

Northern Ireland

UK

Telephone: +44 (0)2890 632718

Abstract

MicroRNAs (miRNAs) bind to complementary sequences within the 3′ untranslated region (UTR) of mRNAs from hundreds of target genes, leading either to mRNA degradation or suppression of translation. We found that a mutation in the seed region of miR-184 (miR184) is responsible for familial severe keratoconus combined with early-onset anterior polar cataract, by deep sequencing of a linkage region known to contain the mutation. The mutant form fails to compete with miR-205 (miR205) for overlapping target sites on the 3′ UTRs of *INPPL1* and *ITGB4*. Although these target genes and miR-205 are expressed widely, the phenotype is restricted to the cornea and lens because of the very high expression of miR-184 in these tissues. Our finding highlights the tissue-specificity of a gene network regulated by a miRNA. Awareness of the important function of miRNAs may aid identification of susceptibility genes and new therapeutic targets for treatment of both rare and common diseases.

Keratoconus (MIM 148300) is a non-inflammatory thinning of the central cornea, which results in cone-shaped protrusion of the cornea, alteration in refractive power, reduced visual acuity and image distortion. It is the most common corneal dystrophy, with an incidence of 1 in 2,000[1] and is a major reason for corneal transplantation.[2] Keratoconus is usually inherited as an autosomal dominant trait with variable expression. Mutations in the visual system homeobox 1 gene (*VSX1* [MIM 605020]) have been identified in patients with keratoconus, however their role in causing disease is controversial.[3, 4] The

pathological mechanism behind keratoconus is poorly understood, but evidence points towards dysregulation of apoptosis.[5, 6]

Small (19-25 nucleotide) regulatory strands of RNA, named microRNAs (miRNAs), bind to complementary sequences, usually in the 3′ UTR of mRNA of target genes, leading to degradation of the mRNA or suppression of translation.[7] As part of a RNA-induced silencing complex, each miRNA may target mRNA from hundreds of genes.[8] Tissue-specific expression of miRNAs may affect the abundance of proteins in different organs and their component parts.

Within the eye, miR-184 (encoded by *MIR184* [MIM 613146]) is expressed in the central corneal epithelial basal and suprabasal cells, and in the lens epithelium.[9, 10] In both tissues it is the most abundant miRNA. MiR-205 is a widely-expressed epithelial miRNA encoded by *MIR205* (MIM 613147). One observed action of miR-184 is the competitive inhibition of the binding of miR-205 to mRNA of the inositol polyphosphate phosphatase-like 1 gene (*INPPL1*, also known as *SHIP2* [MIM 600829]).[11] Through this mechanism, miR-184 prevents knock-down by miR-205 and rescues INPPL-1 production. Ultimately, this sustains levels of phosphorylated AKT and phosphorylated BCL-2-associated death promoter (BAD), which regulate apoptosis.[11]

We investigated the cause of disease in a Northern Irish family in which 18 of 38 individuals from three generations were affected by an autosomal dominant form of severe anterior keratoconus and early-onset anterior polar cataract. We previously mapped the disease locus in this family to a 5.5 Mb region of chromosome 15q22-q25 and excluded many positional candidate genes by conventional sequencing.[12, 13]

Recently, we enriched for all genes within the region by sequence capture. A custom sequence capture array (Roche NimbleGen, Madison, Wisconsin, USA) was designed to capture 5 Mb of the 5.5 Mb linkage region at 15q22-q25 (a repetitive gene-devoid 0.5 Mb region was excluded). The array was designed using the Sequence Search and Alignment by Hashing Algorithm and comprised 385,000 unique probes.[14] Three study DNA samples were captured: one affected family member, and two pooled DNA samples from 7 affected and 6 unaffected family members, respectively. DNA samples were enriched for the targeted sequences using the manufacturer's protocols. Briefly, 21 µg aliquots were fragmented and hybridized to the array followed by ligation-mediated PCR amplification of the enriched fragmented DNA pool. Five micrograms of amplified enriched DNA underwent massively parallel sequencing on a Genome Analyzer II (Illumina, San Diego, California, USA) with a single sample per flow cell to generate single-end reads of 40 bp (GATC Biotech, Konstanz, Germany).

Sequence data were converted from Solexa to Sanger standard format by use of Maq 0.7.1 and aligned to the NCBI v37 reference sequence using the BWA 0.5.9 short alignment algorithm.[15] Sorting, indexing and removal of duplicates were performed with Samtools 0.1.14.[16] Picard 1.43 was used to edit read groups information. Functions of Genome Analysis Toolkit (GATK)[17] were used to recalibrate base calls, realign reads at the sites of possible insertions, duplications and deletions, and call polymorphisms (Unified Genotyper). Version 130 of dbSNP and the 4th August 2010 release of Dindel data for Europeans from the 1000 genomes project were employed for realignment. VCFtools 0.1.5 was used to compare variant calls from the three sample groups. Sequence was visualized with Integrative Genomics Viewer 1.5.[18] We used GATK to

annotate the polymorphisms with gene information from the RefSeq Genes track (made by the Genome Sequencing and Analysis group at the Broad Institute from the UCSC RefSeq Genes Track, itself derived from NCBI mRNA reference sequences collection; see Web Resources). Polymorphisms outside gene exons were excluded from further analyses. All variant calls from the three samples were entered into a database, which was queried for instances where the affected individual and affected pool shared any genetic variation that was not present in the unaffected pool. Mean depth of coverage was 23-28 reads in each sample, with 70-77% having >15x coverage. Twenty-six variants (25 single nucleotide variants and one deletion of two bases) within exons and untranslated regions of coding and non-coding genes were identified that fitted this pattern (Table 1). We searched dbSNP and the 1000 Genomes Project data release of May 2011 for these polymorphisms. All but two SNPs were already known and were identified in European populations at a frequency of greater than 7.5% and were thus excluded from further consideration. A deletion of two bases was not recorded in dbSNP or the 1000 Genomes Project. Three possible causative mutations were therefore identified (Table 2).

We searched public databases for information about the function and expression of *MIR184*, *DNAJA4* and *IREB2*. MiR-184 is the most abundantly expressed microRNA in the corneal and lens epithelia, and is known to be involved in the regulation of protein levels in those tissues.[9] The novel heterozygous C-to-T transition (r.57c>u) within miR-184 (Figure 1) is in the central nucleotide of the functionally essential seven-base miRNA seed region. *DNAJA4* is expressed in a wide range of tissues. Its product is a chaperone molecule involved in cholesterol biosynthesis.[19] The two bases are deleted

from the start codon of an alternatively spliced first exon. The deletion is predicted to prevent formation of isoform 3 of DNAJA4 from this allele. Relatively little is known about this gene, but it is not known to have any important role in the eye. *IREB2* (MIM 147582) encodes an iron-responsive element binding protein which regulates iron metabolism.[20] The mutation in *IREB2* in the 3′ UTR is not predicted by MicroCosm Targets to interact with any miRNA. [21, 22]

In light of its role and specific abundance in the cornea and lens, the mutation altering the seed region of miR-184 (r.57c>u) was the compelling candidate of the three previously unknown variants detected within exons. The gene is conserved in all 65 species known to have a copy of miR-184 (Figure 2A). We performed conventional sequencing of *MIR184* (Table S1) in 167 unscreened controls and found no mutation within the mature miRNA. The miR-184 (r.57c>u) mutation was not reported in the 1,094 individuals in the 1,000 Genomes Project data release of May 2011.[23] Predictions of RNA folding using Mfold[24] suggest that the mutation does not destabilize the secondary structure of the mir-184 pre-miR (Figure 2B).

The known competition between miR-184 and miR-205 for the 3′ UTR of *INPPL1* (Figure 2C) facilitated a relatively straightforward functional assessment for miR-184 (r.57c>u). *INPPL1* is expressed constitutively by HeLa cells, but neither miR-184 nor miR-205 is expressed.[25, 26] We used computational target prediction (the MicroCosm Targets v.5[21, 22] implementation of the miRanda algorithm [27]) to search for other instances where miR-184 and miR-205 had overlapping target sites in a 3′ UTR. This yielded only one other target, integrin beta 4 (*ITGB4* [MIM 147557]*),* which is the main

structural protein of hemidesmosomes that connect corneal basal epithelial cells to the basement membrane.[28]

We adapted Yu *et al*.'s experiment[11] to test the ability of the mutant (r.57u) and wild-type miR-184 to interfere with miR-205 knockdown of *INPPL1* and *ITGB4* transcripts in HeLa cells, by immunohistochemical staining and by western blotting.

Blunt-ended double-stranded miRNA mimics for the predominant isoforms of miR-184 and miR-205 (Figure S1), and for the mutant miR-184 (r.57u) were synthesized by Invitrogen (Table S2). HeLa cells (which express *INPPL1* and *ITGB4*, but not miR-184 or miR-205) were grown to 70% confluence in 24-well plates in DMEM medium without antibiotics, and transfected with miRNA mimics (20 nmol/L) using Santa Cruz transfection reagent according to the standard protocol. Cells were cultured for 72 h before harvesting for western blotting and staining with anti-INPPL1 (NEBiolabs; #2839), anti-ITGB4 antibody (Abcam; #29042) or anti-α-tubulin (Abcam; #4074) at a dilution of 1:1000. Donkey anti-rabbit and chicken anti-mouse HRP-linked secondary antibodies were used for western blotting and donkey anti-rabbit FITC-linked secondary antibodies (Abcam) with Alexa Fluor-555-labelled phalloidin (Invitrogen) used for immunofluorescence. Western blots were performed for five sets of transfections. Luminescence was detected and quantified using a UVP BioSpectrum AC Imaging System.

Cells from an additional set of transfections were stained with fluorescently labeled antibodies. Immunofluorescence was detected using an Olympus IX51 microscope and Spot Diagnostics V4.1 (Diagnostic Instruments Inc.) software. Semi-quantitative

analysis was carried out on a minimum of 30 cells for each condition using Adobe Photoshop CS3. Statistical analyses were carried out using PASW statistics v18.0.0 (SPSS Inc., Chicago, IL, USA) and charts plotted with the gplots package[29] within R v2.10.1.[30]

The levels of INNPL-1 (Figure 3A) and ITGB4 (Figure 3B) in HeLa cells in response to transfection with combinations of synthetic miRNAs was measured by western blotting. Knockdown of INNPL-1 was minimal with miR-184 mimic (4.4%; p=0.03) and negligible with mutant miR-184 mimic (1.8%; p=0.33). Transfection with miR-205 mimic reduced the amount of INPPL-1 detected to 47% of that in control cells which underwent the process of transfection without any synthetic miRNA (p=3.5x10^{-5}). Transfection with miR-205 mimic in combination with wild-type miR-184 mimic resulted in rescue of levels of INPPL-1 to 86% of controls (p=2.5x10^{-3}). However, transfection with miR-205 mimic in combination with mutant miR-184 mimic resulted in failure to rescue INPPL-1 levels (44% vs 47%; p=0.57 compared to miR-205 mimic alone).

Knockdown of ITGB4 was moderate with miR-184 mimic (13%; p=3.4x10^{-4}) and negligible with mutant miR-184 mimic (3%; p=0.24). Transfection with miR-205 mimic reduced the amount of ITGB4 detected to 47% of that in control cells which underwent the process of transfection without any synthetic miRNA (p=2.8x10^{-5}). Transfection with miR-205 mimic in combination with wild-type miR-184 mimic resulted in rescue of levels of ITGB4 to 80% of controls (p=4.0x10^{-3}). However, transfection with miR-205 mimic in combination with mutant miR-184 mimic resulted in failure to rescue ITGB4 levels (44% vs 47%; p=0.50 compared to *miR-205* mimic alone).

Cells transfected with miR-205 mimic combined with either mutant or wild-type miR-184 mimic were stained for INPPL-1 and ITGB4. Cells treated with the mutant miR-184 mimic showed a 37% reduction of INPPL-1 compared to cells treated with wild-type miR-184 mimic (Figures 4A, B and C; $p=1.3x10^{-4}$). Cells treated with the mutant miR-184 mimic showed a 48% reduction of ITGB4 compared to cells treated with wild-type miR-184 mimic (Figure 4D, E and F; $p=7.5x10^{-6}$).

The tissue-specific expression of miR-184 is of prime importance in the phenotypic effects that the mutation causes. Within the cornea, miR-184 expression is restricted to central basal and suprabasal epithelial cells,[9] under which the stromal thinning occurs in keratoconus. Within the lens, the epithelium lies anteriorly and, paralleling the cornea, has less proliferative capacity centrally.[31] This anterior lens epithelium expresses miR-184,[9] adjacent to the site of cataract in the affected family.

In the cornea, ITGB4 forms part of the α6β4 heterodimer, which is the principal component of corneal basal epithelial hemidesmosomes.[28] Following corneal injury, hemidesmosomes in the basal epithelial layer are degraded to allow epithelial cell migration and are subsequently rebuilt. Expression of miR-184 is halted at the site of corneal injury, and returns after healing.[9] Dysregulation of the expression of *ITGB4* in the central cornea (the site of miR-184 expression) may therefore also be important. The stromal keratocytes underlying the site of an injury undergo rapid apoptosis as a defense mechanism.[6] Therefore the role of INPPL-1 in regulation of apoptosis may also be vital in the development of keratoconus and cataract.

Expression of as many as 1,000 genes may be regulated by miR-184, independently or in competition with other miRNAs, which may lead to complex effects on the levels of a large number of proteins. The harmful effects of mutant miR-184 may be mediated through proteins other than INPPL-1 and ITGB4. Among the predicted targets of miR-184 are a major lens transcription factor (*FOXE3* [MIM 601094]) and a major intrinsic protein of eye lens fiber (*MIP* [MIM 154050]), mutations in both of which cause lens abnormalities in humans.[32] The competition between miR-184 and miR-205, identified by Yu *et al,* and confirmed in our study, illustrates the complexity of miRNA action. We do not, at present, know why miR-184 is less effective than miR-205 at knock-down of INPPL-1 and ITGB4. Further studies are required to illuminate the molecular mechanisms involved.

In some cases, myopia is due to a steeply curving cornea. A genome-wide association study identified a small region encompassing *MIR184* as a major myopia locus,[33] and focused on *RASGRF1* (MIM 606600), which is adjacent to *MIR184*. Our finding that a *MIR184* mutation causes keratoconus suggests that this gene warrants further investigation with respect to myopia.

The role of miRNAs in human diseases and possible treatments is a new and expanding field of study. This is the second report of a mutation in a miRNA associated with a human mendelian disease. The previous report identified two mutations in miR-96 that resulted in hereditary deafness in two Spanish families.[34]

Our report demonstrates that variation in miRNAs can cause disease that is specific to the tissue in which the miRNA is expressed. This knowledge may open new lines of

enquiry for those investigating the causes of diseases, and may indeed suggest possible treatments: the therapeutic use of miRNA in eye diseases is a real and noteworthy prospect.

Supplemental Data

Supplemental Data include two tables and one figure and can be found with this article online at http://www.cell.com/ASHG

Acknowledgements

This work was supported by Northern Ireland Research and Development Office RRG grant 4.46 and Fight for Sight grant 1787. DTB was funded by the Public Health Agency (Northern Ireland). We are grateful for the longstanding interest of the family who participated in the study and to the clinicians who recruited and cared for the family. Bioinformatics work was conducted on the QUB High Performance Computing Dell cluster. The study was approved by the Northern Ireland Office for Research Committees and conformed to the tenets of the Declaration of Helsinki. CEW, DAS and AEH designed and oversaw the study. DTB and AEH analyzed massively parallel sequence data, performed conventional sequencing and drafted the manuscript. MC performed all cell experiments. JL analyzed additional genotype data. DPD prepared DNA, and organized sequence capture and massively parallel sequencing experiments. CEW obtained funding. All authors contributed to critical review of the paper.

Web Resources

Online Mendelian Inheritance in Man (OMIM), http://www.omim.org

Mapping and Assembly with Qualities (MAQ), http://maq.sf.net

Burrows-Wheeler Aligner (BWA), http://bio-bwa.sourceforge.net

SAMtools, http://samtools.sourceforge.net

The Genome Analysis Toolkit (GATK), http://www.broadinstitute.org/gatk

Genomic Annotator Data Tables,
http://www.broadinstitute.org/gsa/wiki/index.php/Genomic_Annotator_Data_Tables

VCFtools, http://vcftools.sourceforge.net

Integrative Genomics Viewer (IGV), http://www.broadinstitute.org/software/igv

MFold, http://mfold.rna.albany.edu

MicroCosm Targets, http://www.ebi.ac.uk/enright-srv/microcosm

1000 Genomes Project, http://www.1000genomes.org

R, http://www.r-project.org

gplots, http://cran.r-project.org/web/packages/gplots

References

1. Kennedy, R.H., Bourne, W.M., and Dyer, J.A. (1986). A 48-year clinical and epidemiologic study of keratoconus. Am. J. Ophthalmol. 101, 267-273.

2. Ghosheh, F.R., Cremona, F.A., Rapuano, C.J., Cohen, E.J., Ayres, B.D., Hammersmith, K.M., Raber, I.M., and Laibson, P.R. (2008). Trends in penetrating keratoplasty in the United States 1980-2005. Int. Ophthalmol. 28, 147-153.

3. Heon, E., Greenberg, A., Kopp, K.K., Rootman, D., Vincent, A.L., Billingsley, G., Priston, M., Dorval, K.M., Chow, R.L., McInnes, R.R. *et al*. (2002). VSX1: a gene for posterior polymorphous dystrophy and keratoconus. Hum. Mol. Genet. 11, 1029-1036.

4. Dash, D.P., George, S., O'Prey, D., Burns, D., Nabili, S., Donnelly, U., Hughes, A.E., Silvestri, G., Jackson, J., Frazer, D. *et al*. (2010). Mutational screening of VSX1 in keratoconus patients from the European population. Eye (Lond) 24, 1085-1092.

5. Kim, W.J., Rabinowitz, Y.S., Meisler, D.M., and Wilson, S.E. (1999). Keratocyte apoptosis associated with keratoconus. Exp. Eye Res. 69, 475-481.

6. Wilson, S.E., Chaurasia, S.S., and Medeiros, F.W. (2007). Apoptosis in the initiation, modulation and termination of the corneal wound healing response. Exp. Eye Res. 85, 305-311.

7. Lee, R.C., Feinbaum, R.L., and Ambros, V. (1993). The C. elegans heterochronic gene lin-4 encodes small RNAs with antisense complementarity to lin-14. Cell 75, 843-854.

8. Meola, N., Gennarino, V.A., and Banfi, S. (2009). microRNAs and genetic diseases. Pathogenetics 2, 7.

9. Ryan, D.G., Oliveira-Fernandes, M., and Lavker, R.M. (2006). MicroRNAs of the mammalian eye display distinct and overlapping tissue specificity. Mol. Vis. 12, 1175-1184.

10. Karali, M., Peluso, I., Gennarino, V.A., Bilio, M., Verde, R., Lago, G., Dolle, P., and Banfi, S. (2010). miRNeye: a microRNA expression atlas of the mouse eye. BMC Genomics 11, 715.

11. Yu, J., Ryan, D.G., Getsios, S., Oliveira-Fernandes, M., Fatima, A., and Lavker, R.M. (2008). MicroRNA-184 antagonizes microRNA-205 to maintain SHIP2 levels in epithelia. Proc. Natl. Acad. Sci. U. S. A. 105, 19300-19305.

12. Hughes, A.E., Dash, D.P., Jackson, A.J., Frazer, D.G., and Silvestri, G. (2003). Familial keratoconus with cataract: linkage to the long arm of chromosome 15 and exclusion of candidate genes. Invest. Ophthalmol. Vis. Sci. 44, 5063-5066.

13. Dash, D.P., Silvestri, G., and Hughes, A.E. (2006). Fine mapping of the keratoconus with cataract locus on chromosome 15q and candidate gene analysis. Mol. Vis. 12, 499-505.

14. Ning, Z., Cox, A.J., and Mullikin, J.C. (2001). SSAHA: a fast search method for large DNA databases. Genome Res. 11, 1725-1729.

15. Li, H., and Durbin, R. (2009). Fast and accurate short read alignment with Burrows-Wheeler transform. Bioinformatics 25, 1754-1760.

16. Li, H., Handsaker, B., Wysoker, A., Fennell, T., Ruan, J., Homer, N., Marth, G., Abecasis, G., Durbin, R., and 1000 Genome Project Data Processing Subgroup. (2009). The Sequence Alignment/Map format and SAMtools. Bioinformatics 25, 2078-2079.

17. McKenna, A., Hanna, M., Banks, E., Sivachenko, A., Cibulskis, K., Kernytsky, A., Garimella, K., Altshuler, D., Gabriel, S., Daly, M. *et al*. (2010). The Genome Analysis Toolkit: a MapReduce framework for analyzing next-generation DNA sequencing data. Genome Res. 20, 1297-1303.

18. Robinson, J.T., Thorvaldsdottir, H., Winckler, W., Guttman, M., Lander, E.S., Getz, G., and Mesirov, J.P. (2011). Integrative genomics viewer. Nat. Biotechnol. 29, 24-26.

19. Robichon, C., Varret, M., Le Liepvre, X., Lasnier, F., Hajduch, E., Ferre, P., and Dugail, I. (2006). DnaJA4 is a SREBP-regulated chaperone involved in the cholesterol biosynthesis pathway. Biochim. Biophys. Acta 1761, 1107-1113.

20. Meyron-Holtz, E.G., Ghosh, M.C., and Rouault, T.A. (2004). Mammalian tissue oxygen levels modulate iron-regulatory protein activities in vivo. Science 306, 2087-2090.

21. Enright, A.J., John, B., Gaul, U., Tuschl, T., Sander, C., and Marks, D.S. (2003). MicroRNA targets in Drosophila. Genome Biol. 5, R1.

22. Enright Lab. (2011). MicroCosm Targets Version 5, http://www.ebi.ac.uk/enright-srv/microcosm/htdocs/targets/.

23. 1000 Genomes Project Consortium. (2010). A map of human genome variation from population-scale sequencing. Nature 467, 1061-1073.

24. Zuker, M. (2003). Mfold web server for nucleic acid folding and hybridization prediction. Nucleic Acids Res. 31, 3406-3415.

25. Barad, O., Meiri, E., Avniel, A., Aharonov, R., Barzilai, A., Bentwich, I., Einav, U., Gilad, S., Hurban, P., Karov, Y. *et al*. (2004). MicroRNA expression detected by oligonucleotide microarrays: system establishment and expression profiling in human tissues. Genome Res. 14, 2486-2494.

26. Prasad, N.K., and Decker, S.J. (2005). SH2-containing 5'-inositol phosphatase, SHIP2, regulates cytoskeleton organization and ligand-dependent down-regulation of the epidermal growth factor receptor. J. Biol. Chem. 280, 13129-13136.

27. John, B., Enright, A.J., Aravin, A., Tuschl, T., Sander, C., and Marks, D.S. (2004). Human MicroRNA targets. Plos Biology 2, e363.

28. Nishida, T., and Saika, S. (2011). Cornea and Sclera: Anatomy and Physiology. In. Cornea, J. H. Krachmer. ed.(St. Louis, Mo: Mosby/Elsevier), p.17.

29. Warnes, G.R. (2010). gplots: Various R programming tools for plotting data.

30. R Development Core Team. (2009). R: A Language and Environment for Statistical Computing (Vienna, Austria: R Foundation for Statistical Computing).

31. Dai, E., and Boulton, M.E. (2009). Basic Science of the lens. In. Ophthalmology, M. Yanoff and J. S. Duker. ed.(Edinburgh: Mosby/Elselvier), p.381.

32. Bremond-Gignac, D., Bitoun, P., Reis, L.M., Copin, H., Murray, J.C., and Semina, E.V. (2010). Identification of dominant FOXE3 and PAX6 mutations in patients with congenital cataract and aniridia. Mol. Vis. 16, 1705-1711.

33. Hysi, P.G., Young, T.L., Mackey, D.A., Andrew, T., Fernandez-Medarde, A., Solouki, A.M., Hewitt, A.W., Macgregor, S., Vingerling, J.R., Li, Y.J. *et al*. (2010). A genome-wide association study for myopia and refractive error identifies a susceptibility locus at 15q25. Nat. Genet. 42, 902-905.

34. Mencia, A., Modamio-Hoybjor, S., Redshaw, N., Morin, M., Mayo-Merino, F., Olavarrieta, L., Aguirre, L.A., del Castillo, I., Steel, K.P., Dalmay, T. *et al*. (2009). Mutations in the seed region of human miR-96 are responsible for nonsyndromic progressive hearing loss. Nat. Genet. 41, 609-613.

Legends to figures

Figure 1. Multiple alignment of massively parallel sequence reads spanning the seed region of miR-184 from (A) a single individual affected with familial keratoconus and cataract, (B) a pool of 7 affected members of the same family and (C) a pool of 6 unaffected members of the same family. All nucleotides that vary from the reference sequence, shown below, are indicated. Read depth and heterozygosity are designated at the top of each column.

Figure 2. Variants of miR-184 and conservation across species; structure of miR-184, miR-205 and mutant miR-184; Interactions of miR-184 and miR-205. (A) Multiple alignment of miR-184 sequences from different vertebrate species. The mutation site (miR-184 r.57c>u; blue arrow) is fully conserved across all species. Changes from the human reference sequence are shown in green type, the mature miRNAs are shown in red type, with the seed regions in bold. hsa, *Homo sapiens*; ptr, *Pan troglodytes*; ppy, *Pongo pygmaeus*; mne, *Macaca nemestrina*; mdo, *Monodelphis domestica*; gga, *Gallus gallus*; ssc, *Sus scrofa*; rno, *Rattus norvegicus*; mmu, *Mus musculus*; xtr, *Xenopus tropicalis*; dre, *Danio rerio*. Fifty-four additional species showed full conservation of the mature miR-184 sequence. (B) Secondary structures and free energies of wild type miR-184, mutant miR-184 (r.57u) predicted by Mfold. (C) Target sites of miR-184 and miR-205 in the 3' UTRs of *INPPL1* and *ITGB4* predicted by MicroCosm with energies shown in kcal/mol.

Figure 3. Western blot of INPPL-1 and ITGB4. Knockdown for miRNAs was performed in HeLa cells. Signal strengths are shown for INPPL-1 and ITGB4 relative to a sham transfected control, all normalized for α-tubulin loading. One representative image is shown from five replicated experiments. (A) There was no rescue of miR-205 knockdown of INPPL-1 by the mutant miR-184 mimic compared to wild-type miR-184 mimic. (B) There was no rescue of miR-205 knockdown of ITGB4 by the mutant miR-184 mimic compared to wild-type miR-184 mimic.

Figure 4. Immunofluorescence staining of INPPL-1, ITGB4 and actin. Representative micrographs showing (A and B) INPPL-1 (green) and actin (red) for cells transfected with (A) miR-184 mimic and miR-205 mimic and (B) mutant miR-184 and miR-205. Scale bar: 50 μm. (C) Semi-quantitative analysis of mutant *miR-184* knockdown relative to wild-type miR-184, both with miR-205 and standardized for actin. Representative micrographs showing (D and E) ITGB4 (green) and actin (red) for cells knocked down with (D) miR-184 mimic and miR-205 mimic and (E) mutant miR-184 and miR-205. Scale bar: 50 μm. (F) Semi-quantitative analysis of mutant *miR-184* knockdown relative to wild-type miR-184, both with miR-205 and standardized for actin.

Table 1. Annotation of massively parallel sequence. Genetic variants detected in both affected individual and affected pool, but not in unaffected pool, categorized by site.

Site of Variant	Coding Gene		Non-coding Gene	
	Total	Known	Total	Known
Coding sequence	9	9	5	4
5′ or 3′ UTR	12	10	-	-

Table 2. Novel exonic variants.

Gene	Sequence Variant
DNAJA4	g.2099_2100delAT (NC_000015)
IREB2	c.*2043G>T (NM_004136)
MIR184	r.57c>u (NR_029705)

Figure 1

Figure 2

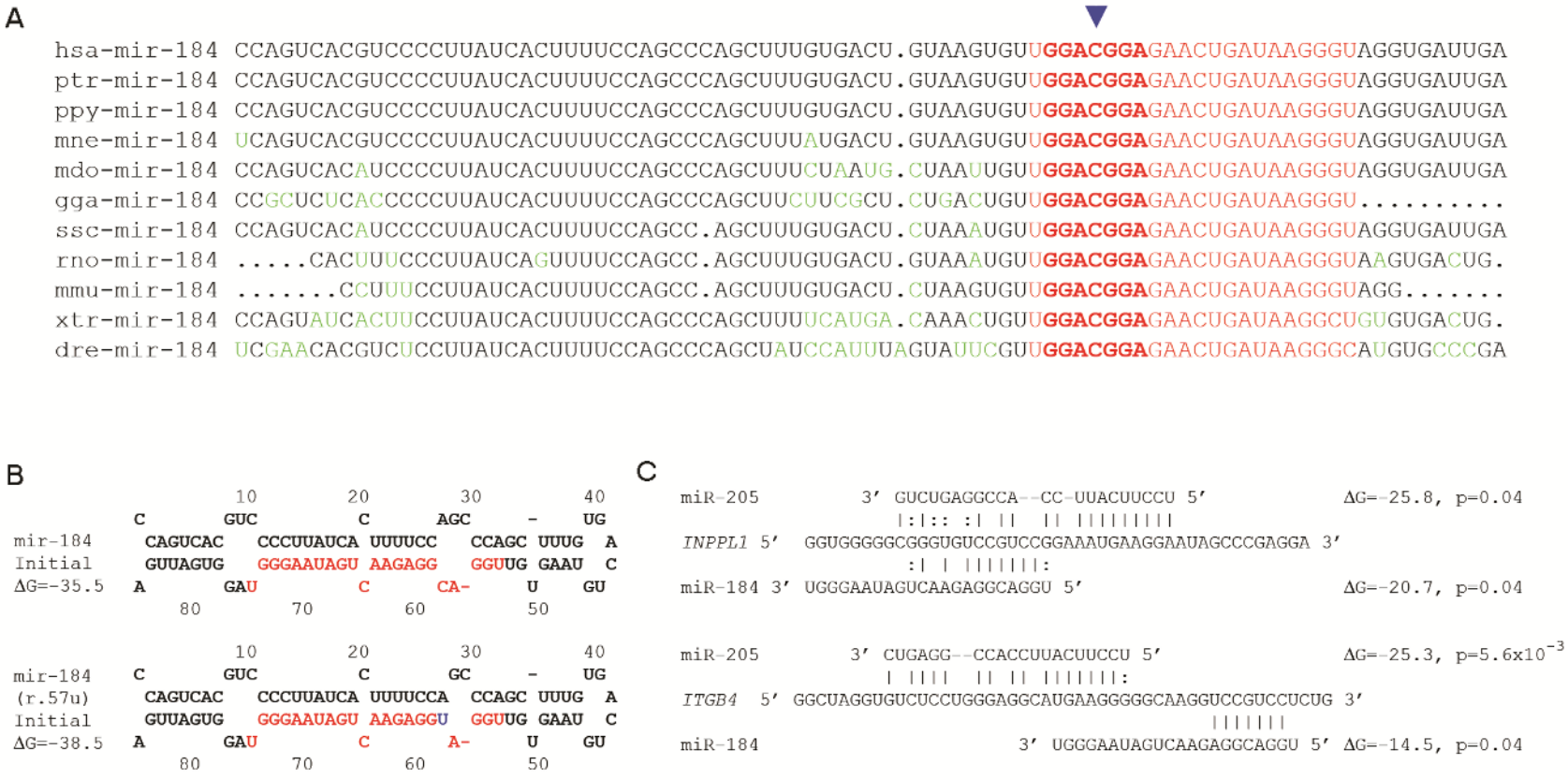
A
hsa-mir-184 CCAGUCACGUCCCCUUAUCACUUUUCCAGCCCAGCUUUGUGACU.GUAAGUGUUGGACGGAGAACUGAUAAGGGUAGGUGAUUGA
ptr-mir-184 CCAGUCACGUCCCCUUAUCACUUUUCCAGCCCAGCUUUGUGACU.GUAAGUGUUGGACGGAGAACUGAUAAGGGUAGGUGAUUGA
ppy-mir-184 CCAGUCACGUCCCCUUAUCACUUUUCCAGCCCAGCUUUGUGACU.GUAAGUGUUGGACGGAGAACUGAUAAGGGUAGGUGAUUGA
mne-mir-184 UCAGUCACGUCCCCUUAUCACUUUUCCAGCCCAGCUUUAUGACU.GUAAGUGUUGGACGGAGAACUGAUAAGGGUAGGUGAUUGA
mdo-mir-184 CCAGUCACAUCCCCUUAUCACUUUUCCAGCCCAGCUUUCUAAUG.CUAAUUGUUGGACGGAGAACUGAUAAGGGUAGGUGAUUGA
gga-mir-184 CCGCUCUCACCCCCUUAUCACUUUUCCAGCCCAGCUUCUUCGCU.CUGACUGUUGGACGGAGAACUGAUAAGGGU..........
ssc-mir-184 CCAGUCACAUCCCCUUAUCACUUUUCCAGCC.AGCUUUGUGACU.CUAAAUGUUGGACGGAGAACUGAUAAGGGUAGGUGAUUGA
rno-mir-184 .....CACUUUCCCUUAUCAGUUUUCCAGCC.AGCUUUGUGACU.GUAAAUGUUGGACGGAGAACUGAUAAGGGUAAGUGACUG.
mmu-mir-184 .......CCUUUCCUUAUCACUUUUCCAGCC.AGCUUUGUGACU.CUAAGUGUUGGACGGAGAACUGAUAAGGGUAGG.......
xtr-mir-184 CCAGUAUCACUUCCUUAUCACUUUUCCAGCCCAGCUUUUCAUGA.CAAACUGUUGGACGGAGAACUGAUAAGGCUGUGUGACUG.
dre-mir-184 UCGAACACGUCUCCUUAUCACUUUUCCAGCCCAGCUAUCCAUUUAGUAUUCGUUGGACGGAGAACUGAUAAGGGCAUGUGCCCGA
B
10 20 30 40
C GUC C AGC - UG
mir-184 CAGUCAC CCCUUAUCA UUUUCC CCAGC UUUG A
Initial GUUAGUG GGGAAUAGU AAGAGG GGUUG GAAU C
ΔG=-35.5 A GAU C CA- U GU
80 70 60 50
10 20 30 40
mir-184 C GUC C GC - UG
(r.57u) CAGUCAC CCCUUAUCA UUUUCCA CCAGC UUUG A
Initial GUUAGUG GGGAAUAGU AAGAGGU GGUUG GAAU C
ΔG=-38.5 A GAU C A- U GU
80 70 60 50
C
miR-205 3′ GUCUGAGGCCA--CC-UUACUUCCU 5′ ΔG=-25.8, p=0.04
INPPL1 5′ GGUGGGGGCGGGUGUCCGUCCGGAAAUGAAGGAAUAGCCCGAGGA 3′
miR-184 3′ UGGGAAUAGUCAAGAGGCAGGU 5′ ΔG=-20.7, p=0.04
miR-205 3′ CUGAGG--CCACCUUACUUCCU 5′ ΔG=-25.3, p=5.6x10-3
ITGB4 5′ GGCUAGGUGUCUCCUGGGAGGCAUGAAGGGGGCAAGGUCCGUCCUCUG 3′
miR-184 3′ UGGGAAUAGUCAAGAGGCAGGU 5′ ΔG=-14.5, p=0.04

Figure 3

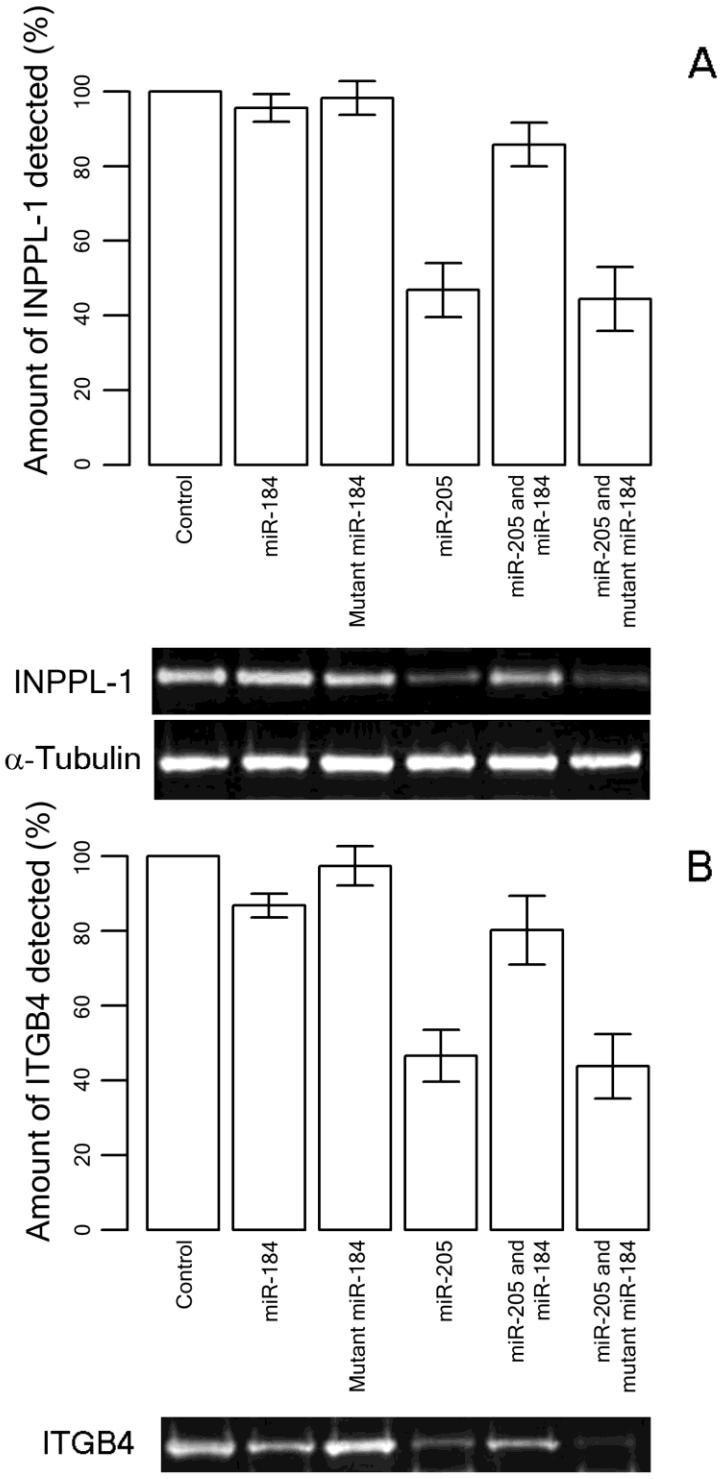
A
Amount of INPPL-1 detected (%)
0
20
40
60
80
100
Control
miR-184
Mutant miR-184
miR-205
miR-205 and miR-184
miR-205 and mutant miR-184
INPPL-1
α-Tubulin
B
Amount of ITGB4 detected (%)
0
20
40
60
80
100
Control
miR-184
Mutant miR-184
miR-205
miR-205 and miR-184
miR-205 and mutant miR-184
ITGB4

Figure 4

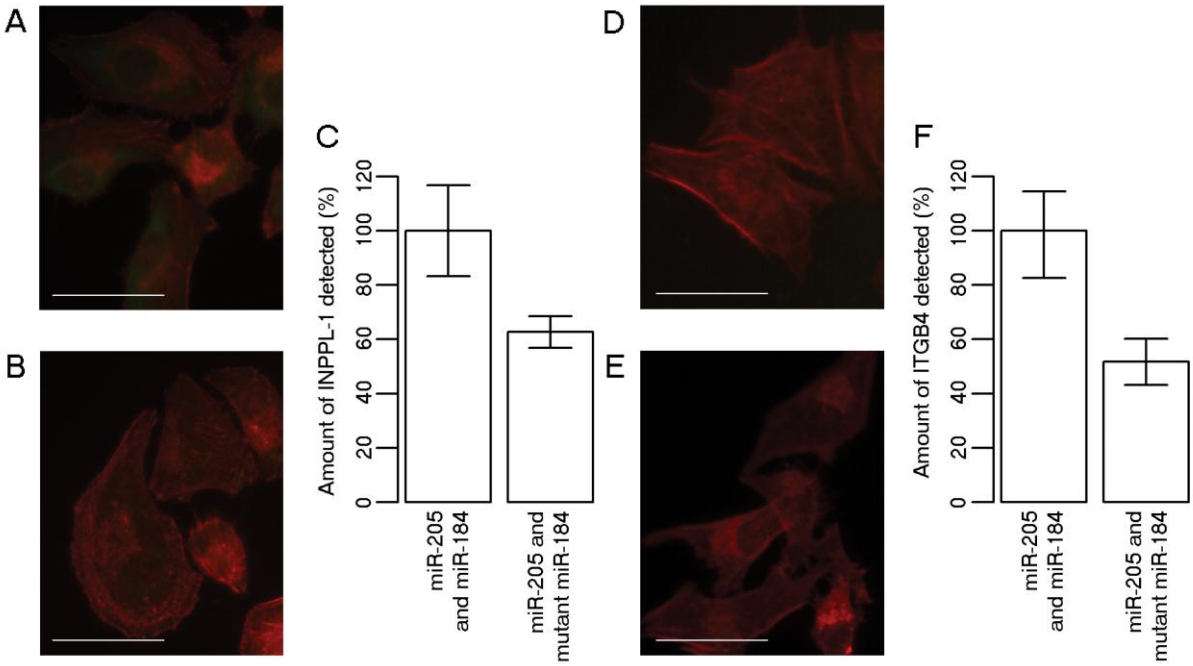
A
B
C
Amount of INPPL-1 detected (%)
0
20
40
60
80
100
120
miR-205 and miR-184
miR-205 and mutant miR-184
D
E
F
Amount of ITGB4 detected (%)
0
20
40
60
80
100
120
miR-205 and miR-184
miR-205 and mutant miR-184

Mutation altering the miR-184 seed region causes familial keratoconus with cataract

Supplementary Data

Figure S1. Relative abundance of isomiRs of miR-184 and miR-205

Counts of isomiR sequencing data for the major and minor forms of miR-184 and miR-205 taken from miRBase (http://www.mirbase.org/) accessed 19 August 2011. MiR mimics were based on the sequence of the major form of miR-184 and of miR-205.

Primer Name	Sequence
MIR184 F	5′-ACGTCCATTTACATCTTGTCCTGC-3′
MIR184 R	5′-ACACAAAGGCTACCCCAGCATCC-3′

Table S1. PCR primer sequences

miRNA mimic	Sequence
miR-184	5′-UGGACGGAGAACUGAUAAGGGU-3′
miR-184 (r.57u)	5′-UGGAUGGAGAACUGAUAAGGGU-3′
miR-205	5′-UCCUUCAUUCCACCGGAGUCUG-3′

Table S2. MiRNA mimic sequences